

# MARL-OT: Multi-Agent Reinforcement Learning Guided Online Fuzzing to Detect Safety Violation in Autonomous Driving Systems

Linfeng Liang  
Macquarie University  
Sydney, NSW, Australia  
linfeng.liang@hdr.mq.edu.au

Xi Zheng  
Macquarie University  
Sydney, NSW, Australia  
James.Zheng@mq.edu.au

## ABSTRACT

Autonomous Driving Systems (ADSs) are safety-critical, as real-world safety violations can result in significant losses. Rigorous testing is essential before deployment, with simulation testing playing a key role. However, ADSs are typically complex, consisting of multiple modules such as perception and planning, or well-trained end-to-end autonomous driving systems. Offline methods, such as the Genetic Algorithm (GA), can only generate predefined trajectories for dynamics, which struggle to cause safety violations for ADSs rapidly and efficiently in different scenarios due to their evolutionary nature. Online methods, such as single-agent reinforcement learning (RL), can quickly adjust the dynamics' trajectory online to adapt to different scenarios, but they struggle to capture complex corner cases of ADS arising from the intricate interplay among multiple vehicles. Multi-agent reinforcement learning (MARL) has a strong ability in cooperative tasks. On the other hand, it faces its own challenges, particularly with convergence. This paper introduces MARL-OT, a scalable framework that leverages MARL to detect safety violations of ADS resulting from surrounding vehicles' cooperation. MARL-OT employs MARL for high-level guidance, triggering various dangerous scenarios for the rule-based online fuzzer to explore potential safety violations of ADS, thereby generating dynamic, realistic safety violation scenarios. Our approach improves the detected safety violation rate by up to 136.2% compared to the state-of-the-art (SOTA) testing technique.

## CCS CONCEPTS

- **Security and privacy** → **Software and application security**;
- **Software and its engineering** → **Search-based software engineering**.

## ACM Reference Format:

Linfeng Liang and Xi Zheng. 2025. MARL-OT: Multi-Agent Reinforcement Learning Guided Online Fuzzing to Detect Safety Violation in Autonomous Driving Systems. In *Proceedings of ACM Conference (Conference'17)*. ACM, New York, NY, USA, 11 pages. <https://doi.org/10.1145/nnnnnnnn.nnnnnnnn>

Permission to make digital or hard copies of all or part of this work for personal or classroom use is granted without fee provided that copies are not made or distributed for profit or commercial advantage and that copies bear this notice and the full citation on the first page. Copyrights for components of this work owned by others than ACM must be honored. Abstracting with credit is permitted. To copy otherwise, or republish, to post on servers or to redistribute to lists, requires prior specific permission and/or a fee. Request permissions from [permissions@acm.org](mailto:permissions@acm.org).

Conference'17, July 2017, Washington, DC, USA

© 2025 Association for Computing Machinery.

ACM ISBN 978-x-xxxx-xxxx-x/YY/MM...\$15.00

<https://doi.org/10.1145/nnnnnnnn.nnnnnnnn>

## 1 INTRODUCTION

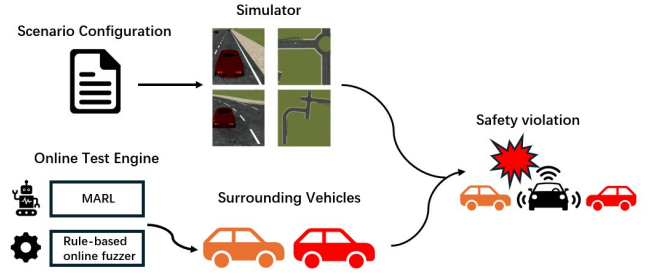


Figure 1: A high-level overview of MARL-OT framework.

Autonomous Driving Systems (ADSs) are complex, typically consisting of multiple modules working together [1, 36] or well-trained end-to-end autonomous driving systems [8] to ensure reliability and safety. Given the critical importance of ADS safety [6], thorough evaluation is essential before real-world deployment [4]. However, real-world testing demands vast driving miles, leading to high costs and time commitments [19]. In contrast, simulation-based testing offers benefits such as controlled environments, the ability to test diverse scenarios, and the creation of dangerous situations without endangering human lives. As a result, researchers have developed various methods for constructing virtual scenarios to assess ADSs [11, 22].

Simulation testing is widely used for ADSs [11, 14, 20, 23], with recent studies showing that scenario-based testing can generate critical corner cases through both online and offline approaches [13, 20, 22, 37]. Offline approaches, such as GA, rely on evolutionary processes across generations to generate predefined violation configurations through continuous searching. However, GA struggles to effectively generate trajectories for dynamics, like throttle and steering sequences for vehicles, especially in scenarios with multiple dynamics [20, 37]. This limitation hampers the exploration of the search space, leading to missed critical corner cases [22] (*challenge 1*).

Recent research indicates that online methods, such as RL, are effective for real-time scenario adaptation and corner case generation [13, 18, 22]. Techniques like backward training [18] and surrogate training [22] have been developed to enhance RL agents' convergence. However, in ADS testing context, single-agent systems struggle to detect safety violations resulting from interactions between multiple surrounding vehicles, which are common in real-world accidents (*challenge 2*). Meanwhile, MARL faces significant

convergence challenges, even with rapid convergence techniques, due to the large action and state spaces in simulations and the rarity of violations (*challenge 3*).

This paper introduces a novel method, Multi-Agent RL Online Testing (MARL-OT), to address these challenges. Figure 1 provides an overview of MARL-OT: within a given scenario, MARL-OT uses a pre-trained MARL system for high-level guidance, which converges in 15 minutes. The rule-based fuzzing logic then maps the MARL output to natural driving behavior, triggering various dangerous scenarios for the rule-based online fuzzer to manipulate. This generates natural, realistic driving behaviors for surrounding vehicles and creates cooperative scenarios that lead to safety violations by the ego vehicle. This approach establishes an efficient, scalable pipeline for generating safety violations in ADS. Our approach improves the detected safety violation rate by up to 136.2% compared to the SOTA testing technique. Our contributions are as follows:

- We propose MARL-OT, an adaptive MARL-based online testing tool that detects ego vehicle violations driven by cooperative behaviors among surrounding vehicles.
- We propose a rule-based online fuzzing approach that models driving maneuvers by mapping continuous MARL agent outputs to discrete actions, triggering realistic and smooth rule-based patterns for each surrounding vehicle.
- We conduct extensive experiments across different scenarios and ADSs to demonstrate that our method effectively detects normal, natural, and realistic violations caused by the ego vehicle controlled by ADSs.

This paper is organized as follows: In Section 2, we provide a review and discussion of the related work relevant to our study. Section 3 details the development of our method. In Section 4, we describe the design of our experiments. Section 5 presents the results of our comprehensive experiments based on the methodology outlined in Section 3. In Section 6, we discuss the utility and the future work related to our proposed method. Conclusions are summarized in Section 7.

## 2 RELATED WORK

### 2.1 Search-Based Offline Testing

The efficacy of GA in identifying corner test cases that trigger violations and failures in cyber-physical systems has been well-documented [2, 5, 12, 15, 20, 27, 32, 33]. GA is widely used in search-based software testing, typically as an offline search technique [40].

In [2, 5], new objective functions with multiple test goals were proposed to guide the search for test scenarios to evaluate Advanced Driver Assistance Systems (ADAS). In [12], a search-based method was introduced to test Baidu Apollo's pedestrian detection algorithm [3], manipulating static parameters like weather and the positions of dynamic objects. AV-FUZZER [20] combines global and local fuzzers based on GA to find corner cases in ADSs. AutoFuzz [41] shows that neural networks can enhance GA by using gradients to mutate seeds. ScenoRITA [15] proposes new gene representations for testing scenarios, allowing obstacles to be fully mutable and improving violation detection. Recent work, MOSAT [37], uses GA to manipulate driving maneuver patterns from real-world crash scenarios to better identify violations in ADSs.

These works focus on innovative scenario representations, objective functions, and crossover and mutation operations, generating test scenarios offline. However, due to their evolutionary nature, offline methods struggle to quickly generate action sequences, such as throttle and steering, for ADS, particularly when handling multiple scenarios. Additionally, they limit interactions between dynamic objects and the ego system, reducing the discovery of corner cases. In contrast, we propose an online fuzzer guided by MARL to search dynamic actions online, maximizing the likelihood of rapidly identifying safety violations in a given scenario.

### 2.2 RL-based Online Testing

The effectiveness of RL in generating violation cases for software testing has been well-demonstrated [17, 26]. RL operates as a Markov Decision Process (MDP), involving agents, actions, policies, and rewards in an interactive environment [35]. In an MDP, the agent perceives the current state, takes actions based on a policy, and receives rewards. RL can be used for online testing to dynamically generate corner cases through predefined reward functions [17, 25]. Research indicates that RL-based online testing approaches can control dynamic objects in real-time within test scenarios, exploring a broader range of potential violations [17, 25]. D2RL introduces an RL-based method to fully capture the ADS testing environment, though it requires significant computational resources and long training periods [13]. GARL [22] combines GA and RL to generate diverse scenarios and dynamic trajectories that trigger violations in UAV landing scenarios.

MARL has been widely deployed for both competitive and cooperative tasks, such as in StarCraft [39] and UAV target capture tasks [16]. Compared to single-agent RL, MARL more closely aligns with real-world scenarios, where many accidents result from interactions between multiple vehicles, which can be viewed as cooperative interactions. However, in simulation-based testing, due to the vast action and state spaces and the rarity of violations, MARL faces significant convergence problems. Although previous methods such as backward training [18] and surrogate environment training [22] have been proposed to address the convergence problem, it still remains a challenge to map actions from the simplified training environment to the full simulation in a way that naturally results in real and common safety violations.

To address this, we create simplified scenarios to train MARL agents and apply rule-based fuzzing logic to map the MARL output to driving behavior. We then use a rule-based online fuzzer, triggered by MARL, to generate natural, real-world driving maneuvers that cause safety violations by the ego vehicle.

## 3 METHOD

### 3.1 Overview

Figure 2 illustrates the workflow of the MARL-OT framework. First, within an initialized scenario in the simulator, the current state of each agent is evaluated to determine if it triggers the online fuzzer. If *True*, the online fuzzer selects the appropriate rule-based action pattern that meets the triggered condition as the next action of the surrounding vehicle, continuing until the pattern is completed. If *False*, the state is sent to the pre-trained MARL to determine the agent's movement vector for the next time step. The movement

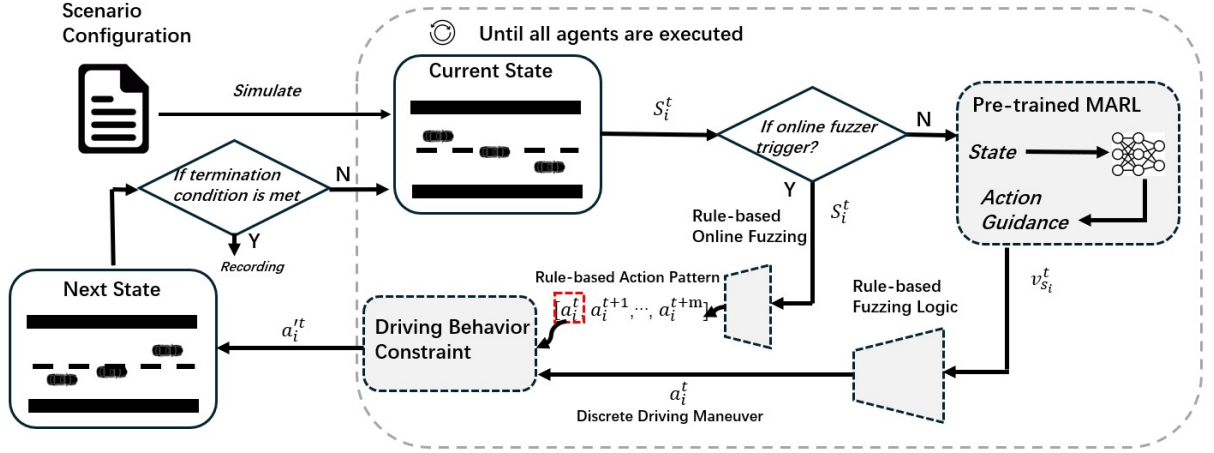


Figure 2: Workflow of MARL-OT.

vector is then mapped to a discrete driving maneuver of the surrounding vehicle through the fuzzing logic, and both the rule-based action pattern and the discrete driving maneuver are regulated by driving behavior constraints to ensure safe driving behavior. This loop continues until all surrounding vehicles have executed their actions. The test ends when the termination condition is met, i.e., the ego vehicle reaches its destination safely or a safety violation occurs. If a safety violation occurs, the case is recorded.

### 3.2 Multi-Agent Reinforcement Learning

In our task, MARL operates with a cooperative objective, where surrounding vehicles aim to keep their positions around the ego vehicle, allowing the online fuzzer to manipulate the surrounding vehicles within the predefined rule-based action pattern. MADDPG [24] has demonstrated strong performance in both performance and convergence, making it an ideal choice for this context.

**3.2.1 State.** The state ( $S$ ) vector encodes the full observation of the environment, which includes positional and motion data for each surrounding vehicle and the ego vehicle. For agent  $i$ , the state is:

$$S_i^t = (P_{s_i,x}^t, P_{s_i,y}^t, v_{s_i,x}^t, v_{s_i,y}^t, \dots, P_{s_{(i+n)},x}^t, P_{s_{(i+n)},y}^t, P_{e,x}^t, P_{e,y}^t) \quad (1)$$

where:

- $P_{s_i,x}^t$  and  $P_{s_i,y}^t$ :  $i$ -th surrounding vehicle's position at  $t$ -th time step,
- $v_{s_i,x}^t$  and  $v_{s_i,y}^t$ : the  $i$ -th surrounding vehicle's length of movement in the  $x$  and  $y$  components at the  $t$ -th time step, respectively. These are initialized with  $[0, 0]$ .
- $P_{e,x}^t$  and  $P_{e,y}^t$ : ego vehicle's position at  $t$ -th time step,
- $n$ : the number of available surrounding vehicles.

**3.2.2 Action Space.** Each surrounding vehicle's action ( $A$ ) at  $t$ -th time step is a continuous 2-tuple vector denote as:

$$A_i^t := \{\Delta v_{s_i,x}^t, \Delta v_{s_i,y}^t\} \quad (2)$$

where:

- $\Delta v_{s_i,x}^t$ : the change of the  $x$ -axis movement length at  $t$ -th time step, with a range of  $[-0.1, 0.1]$ ,
- $\Delta v_{s_i,y}^t$ : the change of the  $y$ -axis movement length at  $t$ -th time step, with a range of  $[0, 0.1]$ .

We enforce  $\Delta v_{s_i,y} > 0$  in our training environment, as vehicles are restricted to forward movement only.

**3.2.3 Reward.** We define a three-phase reward function that encourages cooperative behavior for surrounding vehicles: the first phase incentivizes surrounding vehicles to initially approach the ego vehicle, the second phase promotes encircling the ego vehicle, and the third phase rewards a full enclosure around the ego vehicle. The reward function is as follows:

**Phase 1: Proximity Reward ( $r_{near}$ ).** surrounding vehicles are rewarded for moving closer to the ego vehicle from their initial positions, with alignment of their movement vector toward the ego vehicle:

$$v_{s_i}^t = (v_{s_i,x}^t, v_{s_i,y}^t) \quad (3)$$

$$P_{s_i}^t = (P_{s_i,x}^t, P_{s_i,y}^t) \quad (4)$$

$$P_e^t = (P_{e,x}^t, P_{e,y}^t) \quad (5)$$

$$\cos(\theta_i^t) = \frac{v_{s_i}^t \cdot (P_{s_i}^t - P_e^t)}{\|v_{s_i}^t\|_2 \|P_{s_i}^t - P_e^t\|_2 + 0.001} \quad (6)$$

$$r_{i,near}^t = \|v_{s_i}^t\|_2 \cos(\theta_i^t) \quad (7)$$

**Phase 2: Encirclement Reward.** The surrounding vehicle transitions from proximity to encirclement. Given the complexity of encirclement, we break it down into three stages. The first stage involves the surrounding vehicle tracking the ego vehicle, the second stage involves the surrounding vehicle encircling the ego vehicle, and the third stage involves the surrounding vehicle achieving full enclosure of the ego vehicle. The reward functions are denoted as:

*Stage 1: Tracking Reward ( $r_{\text{track}}$ ).* Surrounding vehicles are rewarded for staying close and beginning to encircle the ego vehicle.

$$\text{if } \sum_{i=1}^n \text{Area}_i^t > \text{Area}_t^t, \quad (8)$$

$$\min_i \|P_{s_i}^t - P_e^t\|_2 \geq d_{\text{enclosure}}$$

$$r_{\text{track}}^t = \begin{cases} -\frac{\sum_{i=1}^n \|P_{s_i}^t - P_e^t\|_2}{\max_{i=1}^n \|P_{s_i}^t - P_e^t\|_2} & \text{if conditions above hold,} \\ 0 & \text{otherwise} \end{cases} \quad (9)$$

*Stage 2: Encircling Reward ( $r_{\text{encircle}}$ ).* As surrounding vehicles form a partial enclosure around the ego vehicle, they receive an additional reward.

$$\text{if } \sum_{i=1}^n \text{Area}_i^t > \text{Area}_t^t, \quad (10)$$

$$\exists i = \{1, 2, \dots, n\}, \|P_{s_i}^t - P_e^t\|_2 < d_{\text{enclosure}}$$

$$r_{\text{encircle}}^t = \begin{cases} -\frac{\log(\sum_{i=1}^n \text{Area}_i^t - \text{Area}_t^t + 1)}{n} & \text{if the conditions above hold,} \\ 0 & \text{otherwise} \end{cases} \quad (11)$$

*Stage 3: Full Enclosure Reward ( $r_{\text{full}}$ ).* A full enclosure around the ego vehicle yields a reward:

$$\text{if } \sum_{i=1}^n \text{Area}_i^t = \text{Area}_t^t, \quad (12)$$

$$\exists i = \{1, 2, \dots, n\}, \|P_{s_i}^t - P_e^t\|_2 > d_{\text{enclosure}}$$

$$r_{\text{full}}^t = \begin{cases} \exp\left(\frac{\sum_{i=1}^n \|P_{s_i}^t - P_e^t\|_2 - \sum_{i=1}^n \|P_{s_i}^{t+1} - P_e^{t+1}\|_2}{n}\right) & \text{if conditions above hold,} \\ 0 & \text{otherwise} \end{cases} \quad (13)$$

where:

- $d_{\text{enclosure}}$ : limitation on the distance required to initiate enclosure.
- $\text{Area}_i^t$ : the area of the triangle formed by the  $i$ -th surrounding vehicle, its adjacent surrounding vehicle, and the ego vehicle.
- $\text{Area}_t^t$ : the total area encompassing all surrounding vehicles.

*Phase 3: Completion Reward ( $r_{\text{finish}}$ ).* Upon successfully encircling the ego vehicle, surrounding vehicles receive a substantial reward:

$$r_{\text{finish}}^t = \begin{cases} \text{I} & \text{if } \sum_{i=1}^n \text{Area}_i^t = \text{Area}_t^t, \\ & \max_i \|P_{s_i}^t - P_e^t\|_2 \leq d_{\text{enclosure}} \\ 0 & \text{otherwise} \end{cases} \quad (14)$$

This final reward reinforces mission completion and concludes the episode, where I is a completion indicator. The overall reward function of each surrounding vehicle at time step  $t$  can be denoted as:

$$\mathbf{R}_i^t = \mu_1 r_{i,\text{near}}^t + \mu_2 (r_{\text{track}}^t + r_{\text{encircle}}^t + r_{\text{full}}^t) + \mu_3 r_{\text{finish}}^t \quad (15)$$

where  $\mu_1$  to  $\mu_3$  are coefficients for each reward component, set empirically.

Additionally, beyond the cooperation reward among agents, we also establish a competition reward for the ego vehicle to encourage it to evade the surrounding vehicle. This reward can be expressed as:

$$r_{\text{ego}}^t = \sum_{i=1}^n \|P_{s_i}^{t+1} - P_e^{t+1}\|_2 - \sum_{i=1}^n \|P_{s_i}^t - P_e^t\|_2 \quad (16)$$

**3.2.4 Training.** Initially, we trained the MARL agents in our customized OpenAI Gym environment [7]. In this environment, the surrounding and ego vehicles can move freely along their output actions without being constrained by road networks. The framework, however, is adaptable and does not depend on a specific simulation environment; as long as the state, action, and reward functions are consistent, training can occur in any simulation setup. The training was conducted on an RTX 3090 GPU and typically completed in 15 minutes.

### 3.3 Modeling Driving Maneuvers

MARL-OT can work with the given scenario, allowing the scenario generator to control most static factors, such as weather, map, and starting and end points for both surrounding and ego vehicles.

To ensure the generated safety violation cases are as realistic as possible, we defined several driving behaviors: *accelerate*, *decelerate*, *brake*, *left lane change*, and *right lane change*. We used pre-defined fuzzing logic to map  $v_{s_i}^t$  to actual driving behavior  $a_i^t$  at  $t$ -th time step. This helps translate the MARL agent's continuous action space into discrete driving behaviors, producing natural driving behavior. The mapping of these driving behaviors is illustrated below:

$$v_{s_i,y}^t \in (0.02, 0.1] \mapsto a_i^t = \text{Accelerate} \quad (17)$$

$$v_{s_i,y}^t \in [0, 0.02] \mapsto a_i^t = \text{Decelerate} \quad (18)$$

$$v_{s_i,y}^t < 0 \mapsto a_i^t = \text{Brake} \quad (19)$$

$$v_{s_i,x}^t < -0.01 \mapsto a_i^t = \text{Left Lane Change} \quad (20)$$

$$v_{s_i,x}^t > 0.01 \mapsto a_i^t = \text{Right Lane Change} \quad (21)$$

### 3.4 Rule-based Online Fuzzing

The MARL works in tandem with the online fuzzer. Once the online fuzzer is triggered, it takes control of the surrounding vehicle. Here, we define several rule-based action patterns for online fuzzing.

**3.4.1 Rule-based Action Pattern.** To maximize the likelihood of violations caused by the ego vehicle, we employ four rule-based action patterns, defined by [37], through a finite-state machine (Figures 3 to 6) for the online fuzzer to manipulate. These patterns are based on previous studies of pre-crash scenarios from NHTSA (National Highway Traffic Safety Administration) [29, 30]. Once an action pattern is triggered, the surrounding vehicle will execute the behavior in the action pattern. The next  $m$  time steps' driving behavior sequence will be generated at time step  $t$  and can be denoted as:

$$[a_i^t, a_i^{t+1}, \dots, a_i^{t+m}] \quad (22)$$

The surrounding vehicle needs to finish the driving behavior in the sequence to finish the action pattern. These rule-based action patterns can be triggered in the following driving scenarios:

- **Ahead action pattern:** Figure 3 shows the behavior model for the ahead action pattern, where the surrounding vehicle is in front of the ego vehicle in the same lane within the safety distance threshold  $D_{\text{safe}}$  which is equal to the lane width. There are three possible driving behaviors once this action pattern is triggered: decelerate, brake, and change to the adjacent lane before returning to the original lane.
- **Side front action pattern:** Figure 4 shows the behavior model for the side front action pattern, where the surrounding vehicle is in front of the ego vehicle but in a different lane (either left front or right front) within the safety distance threshold  $D_{\text{safe}}$ . The surrounding vehicle first changes to the lane where the ego vehicle is located, which is **State A**, then randomly performs one of the following maneuvers with equal probability: decelerate, change lanes, or brake.
- **Behind action pattern:** Figure 5 shows the behavior model for the behind action pattern, where the surrounding vehicle is behind the ego vehicle in the same lane. If the distance between the surrounding vehicle and the ego vehicle,  $D$ , is greater than the safety distance threshold  $D_{\text{safe}}$ , the finite-state machine transitions to **State A**. In this state, the surrounding vehicle will continue accelerating until  $D$  becomes less than  $D_{\text{safe}}$ , at which point it transitions to **State B**. Then, the surrounding vehicle will change to the adjacent lane, which is **State C**, and accelerate until its relative position is in the left front or right front of the ego vehicle.
- **Side behind action pattern:** Figure 6 shows the behavior model for the side behind action pattern, where the surrounding vehicle is behind the ego vehicle in a different lane (either left behind or right behind). When this pattern is triggered, the surrounding vehicle accelerates until it reaches a position in the left front or right front of the ego vehicle.

Multiple agents can trigger these patterns simultaneously. Once triggered, the online fuzzer takes control of the surrounding vehicle until the pattern is completed. The online fuzzer then decides whether to trigger the action patterns again or return control of the surrounding vehicle to the MARL.

### 3.5 Driving Behavior Constraints

We impose several driving behavior constraints to ensure that surrounding vehicles can cooperate smoothly and behave as realistically as possible. Specifically, we enforce two constraints on surrounding vehicles:

- *Constraint 1: surrounding vehicles should not collide with other vehicles during manipulation (including the ego vehicle).*
- *Constraint 2: surrounding vehicles should remain within road boundaries.*

These constraints are applied to both the MARL and the rule-based action pattern. Algorithm 1 illustrates how we apply the constraint to driving behavior. In Algorithm 1, line 1, we first input the maximum distance between surrounding vehicle  $i$  and other vehicles,  $D_{\text{max}}$ , the constraint threshold distance  $D_{\text{constraint}}$  from empirical settings, the discrete driving behavior  $a_t^i$  from the action

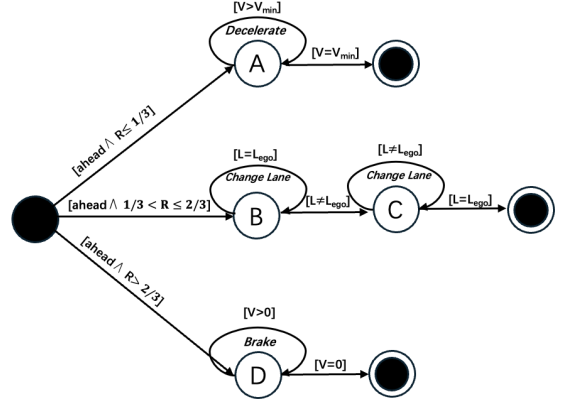


Figure 3: Ahead action pattern [37]

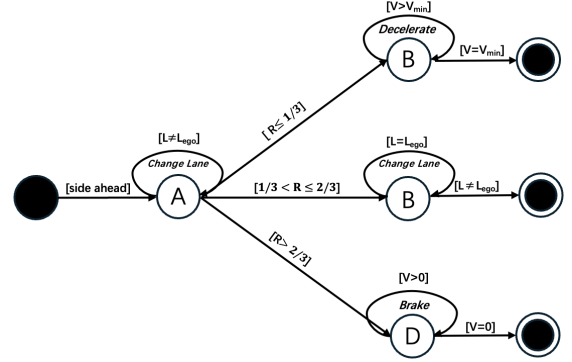


Figure 4: Side front action pattern [37]

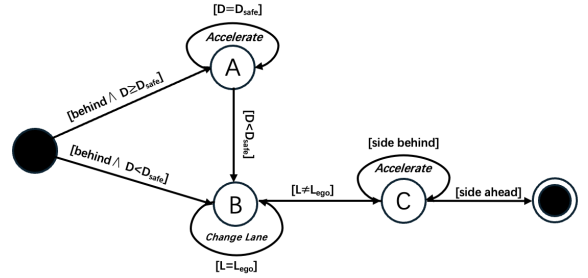


Figure 5: Behind action pattern [37]

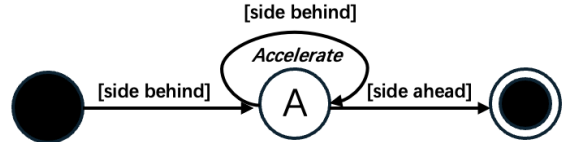


Figure 6: Side behind action pattern [37]

pattern or fuzzing logic at time step  $t$ , and the state of surrounding vehicle  $i$  at time step  $t$ . Then, if  $D_{\max}$  is smaller than  $D_{\text{constraint}}$  or  $S_i^t$  is outside the road boundary (line 3), the surrounding vehicle will execute *brake* at  $t$ -th time step (line 4), or it will output the original  $a_i^t$  (line 6).

---

**Algorithm 1** Driving Behavior Constraints

---

```

1: Input:  $D_{\max}$  (maximum distance between other vehicles),
    $D_{\text{constraint}}$  (constraint threshold distance),  $\text{road\_boundary}$ 
   (road boundary limits),  $a_i^t$  (discrete driving behavior),  $S_i^t$ 
2: Output: Updated discrete driving behavior  $a_i^{t+1}$ 
3: if  $D_{\max} < D_{\text{constraint}}$  or  $S_i^t$  is outside road\_boundary
   then
4:    $a_i^{t+1} = \text{brake}$ 
5: else
6:    $a_i^{t+1} = a_i^t$ 
7: end if

```

---

However, due to the existing motion, there is no guarantee that the surrounding vehicle will stop completely or avoid violating these constraints. This aligns with real-world situations where, even when a driver attempts to brake, it still takes time for the vehicle to come to a complete stop. This is the rationale behind this setting.

## 4 EXPERIMENT

### 4.1 Research Questions

The following research questions (RQs) were assessed to evaluate the performance of MARL-OT:

- RQ1: How effectively does the MARL-OT work across different scenario and ADSs?
- RQ2: How effective is MARL-OT in finding ADS safety violations compared to state-of-the-art techniques?
- RQ3: How realistic are the identified safety violations?

### 4.2 Experiment Setup

We conducted all experiments using Metadrive [21], a powerful simulator that models various road networks and vehicle configurations with high fidelity, including different road types, lane numbers, vehicle types, and setups. Metadrive supports several end-to-end ADSs, including the Intelligent Driver Model (IDM) policy [38] and Proximal Policy Optimization (PPO) Policy [34]. The IDM Policy in Metadrive automatically maintains a safe distance from moving objects and avoids static obstacles, while the PPO Policy, a three-layer MLP with a tanh activation function, is well-trained in the Metadrive environment and effectively handles most driving scenarios. These end-to-end ADSs leverage raw sensing data from the Metadrive simulator, such as LiDAR and camera inputs, to make decisions.

In our experiments, we assume that surrounding vehicles are initially positioned randomly near the ego vehicle within the lane, and their destinations are the same. The default number of agents is set to 3; however, MARL-OT does not limit the number of agents. Each experiment is allocated a test budget of 200 runs and is conducted

5 times, with the averaged results presented. Table 1 indicates the detailed settings of hyperparameter in Section 3.

**Table 1: Hyperparameter Settings**

Component	Parameter	Value
MARL training	Neural network layers	2
	Neurons per layer	128
	Learning rate	0.001
	Initial noise	0.75
	Noise decay	0.999995
	Minimum noise	0.01
	Collision reward (I)	10
	$d_{\text{enclosure}}$	0.3
	$\mu_1$	0.7
	$\mu_2$	0.01
	$\mu_3$	0.5
Simulation	Lane width	3.5
	$D_{\text{safe}}$	3.5
	$D_{\text{constraint}}$	2
	$V_{\min}$	2

### 4.3 Experiment Design

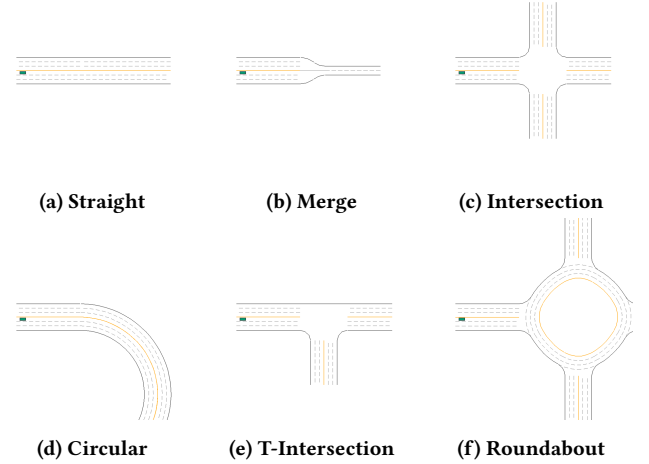


**Figure 7: Example of different road types**

**4.3.1 RQ1.** To evaluate the utility of MARL-OT, we conduct a comprehensive qualitative analysis in Metadrive. First, we perform experiments across all common single road types. Figure 7 illustrates the road types we include, such as **Straight**, **Roundabout**, **Merge**, **T-Intersection**, **Circular**, and **Intersection**. The number of lanes is also a critical factor, as fewer lanes can lead to more crowded traffic, significantly increasing the likelihood of traffic accidents. Therefore, we test each road type with configurations ranging from 2 to 4 lanes.

Beyond single road types, Metadrive supports combinations of these blocks to simulate more complex real-world scenarios. We test combinations of randomly selected sets of 3 blocks, with lane

configurations ranging from 2 to 4 lanes, to form the **MIX** scenario. **MIX** has a significantly longer length than other scenarios. All scenarios are tested with two ADSs, including the IDM Policy [38] and PPO Policy [34] supported by Metadrive [28].

The metric used to assess the utility of MARL-OT is **Safety Violation Rate**. Based on [22], this metric measures the percentage of safety violations detected from the ego vehicle during the test. Here we define **safety violation** [10]:

- **Multiple vehicles crash**: A crash involving the ego vehicle caused by the complex interplay among at least two surrounding vehicles within  $D_{constraint}$ .
- **Abnormal ego vehicle trajectory**: The trajectory of the ego vehicle is extremely abnormal caused by at least two surrounding vehicles within  $D_{constraint}$ , posing a danger on the road and likely to cause an accident.

4.3.2 *RQ2*. In RQ2, we compared MARL-OT with three state-of-the-art (SOTA) baselines in Metadrive: *Random*, GA[20, 37], and *single-agent RL* [22]. To ensure a fair comparison, we set the same number of surrounding vehicles across all baselines, allowing each approach to control these surrounding vehicles. The detailed settings for each baseline are listed below:

- (1) *Random*: In this baseline, the actions of each surrounding vehicle at each time step are randomly selected from the defined driving maneuvers in Section 3.3.
- (2) *GA offline fuzzer* [20, 37]: This baseline leverages a predefined action sequence offline. The action sequences are randomly initialized at the beginning and controlled by NSGA-II [9] through crossover and mutation. The fitness function of the GA is based on safety violations caused by the ego vehicle; if a safety violation occurs, the fitness value of the population is set to 20. The generation size is 10, and the number of generations is 10, aligning with a testing budget of 200.
- (3) *Single-agent RL* [22]: This baseline allows multiple single-agent RL models to control multiple surrounding vehicles independently, without communication between them. The agent's model structure and training environment are the same as MARL-OT; however, all cooperative blocks in MARL are removed to train this single-agent RL. We ensure that the agent has converged during training. The single-agent RL model uses the same rule-based driving maneuvers mapping as described in Section 3.3.

We compared MARL-OT with baselines in all scenarios defined in RQ1 using a 4-lane road and the IDM policy ADS. The 4-lane road presents a larger state space, and the IDM policy ADS is more robust than the PPO policy ADS, creating a greater challenge for the testing technique. In RQ2, we introduce another metric, **TOP-K** [11]. This efficiency metric measures the number of safety violation cases required to identify the first  $K$  safety violation cases, with  $K=5$  in this paper.

4.3.3 *RQ3*. To validate the realism of our generated violations, we conducted a user study. We randomly selected 5 safety violations generated by MARL-OT from each scenario in RQ1 and invited 5 experienced ADS testers to participate. Testers were asked to evaluate the realism of the generated scenarios using a rating scale

from 1 to 5, where 1 indicated 'not realistic' and 5 indicated 'very realistic'.

## 5 RESULT

### 5.1 Utility of MARL-OT (RQ1)

**Table 2: Averaged safety violation rate (%) of ADSs across different scenarios. The number following the ADS indicates the lane count (e.g., L2 denotes 2 lanes). For each road type and lane count, the lowest averaged safety violation rate is highlighted.**

Road Type	IDM L2	PPO L2	IDM L3	PPO L3	IDM L4	PPO L4
<b>Straight</b>	<b>21.1</b>	26.6	<b>15.1</b>	24.6	<b>10.1</b>	19.3
<b>Roundabout</b>	<b>35</b>	40.5	<b>16.8</b>	34.0	<b>10.3</b>	27.7
<b>Merge</b>	32.3	35.5	<b>19.0</b>	26.5	<b>11.1</b>	23.0
<b>T-Intersection</b>	27.3	45.7	<b>12.5</b>	38.3	<b>11.1</b>	30.8
<b>Circular</b>	29.3	32.5	<b>16.5</b>	30.0	<b>14.9</b>	23.3
<b>Intersection</b>	28.5	43.7	<b>14.0</b>	41.5	<b>9.3</b>	26.5
<b>MIX</b>	24.5	32.5	<b>18.5</b>	34.5	<b>13.0</b>	19.0

Table 2 shows the utility results of MARL-OT on 2- to 4-lane roads, demonstrating its effectiveness in identifying safety violations across all scenarios and ADS models. Notably, as the number of lanes increases and the road becomes less crowded, the safety violation rate decreases, which aligns with our intuition.

Then, we find that the IDM policy ADS performs better than the PPO policy ADS in all scenarios, which aligns with the official documentation of Metadrive. The IDM policy incorporates a rule-based approach to maintain distance from moving objects and automatically sidestep static objects, allowing it to make more robust decisions when facing high challenges from MARL-OT. In contrast, the PPO policy is RL-based, and during training, it may not encounter such challenging situations, resulting in lower robustness when tested with MARL-OT.

We manually analyze the collected records and select some typical examples for a case study. Figure 8 presents examples of safety violations from the simulation using a top-down view, and Figure 9 presents two more examples using a 3D view, with each example elaborated on below as a case study.

5.1.1 *Case Study I*. Figure 8a depicts a multiple-vehicle crash in the **Intersection** scenario. The green block represents the ego vehicle, while other blocks represent surrounding vehicles. Initially, the ego vehicle is accelerating, and the front yellow vehicle attempts to change into its lane. The ego vehicle tries to avoid the surrounding vehicle by switching to the left lane, but the yellow vehicle again attempts to change into the same lane. However, two other surrounding vehicles are positioned on the ego vehicle's left side, leaving no space for the ego vehicle to change lanes, resulting in a collision with the yellow lane-changing vehicle.

5.1.2 *Case Study II*. Figure 8b illustrates the **MIX** scenario, where a pink surrounding vehicle is stopped in the lane, and a brown surrounding vehicle is driving on the same lane. As the brown vehicle approaches the pink vehicle, it changes to the adjacent lane to continue moving forward. Unfortunately, after changing lanes, the brown vehicle collides with a red vehicle and comes to a stop.

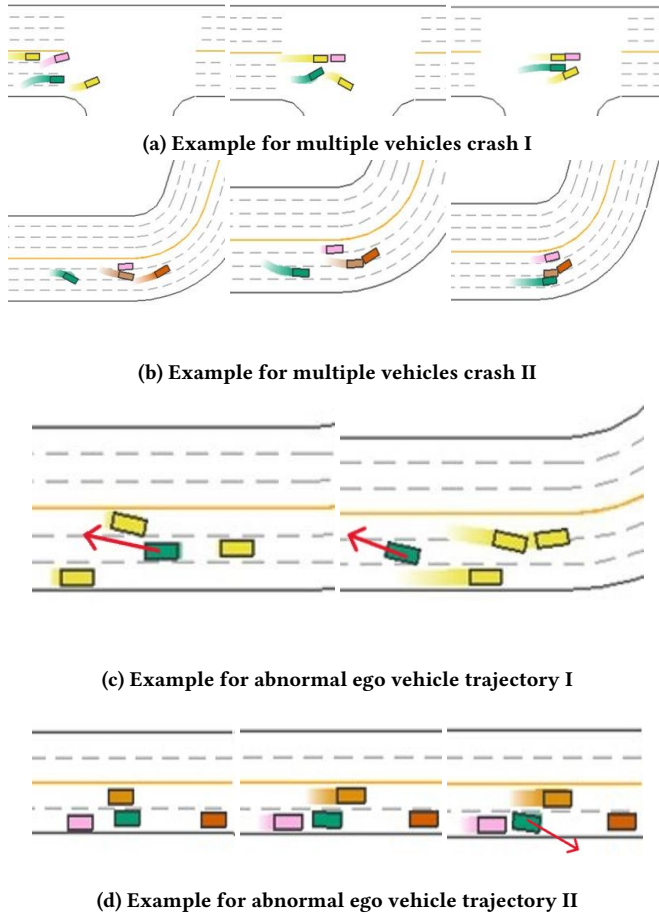


**Figure 8: Examples of safety violation from top-down view simulation**

To avoid the two collided vehicles, the green ego vehicle attempts to change lanes; however, it is too late, and the ego vehicle collides with the stopped brown vehicle.

**5.1.3 Case Study III.** In Figure 8c, the yellow surrounding vehicle to the left of the green ego vehicle is attempting to change into the same lane. Additionally, another yellow surrounding vehicle is positioned ahead of the ego vehicle. The ego vehicle makes an abnormal and dangerous decision to reverse. If there were a vehicle behind the ego vehicle, this could likely result in a collision. In some countries, reversing on the road is strictly prohibited [31].

**5.1.4 Case study IV.** In Figure 8d, a brown surrounding vehicle is passing the green ego vehicle quickly, while a pink surrounding vehicle behind the ego vehicle is accelerating and approaching it. A red surrounding vehicle is stopped ahead of the ego vehicle. In this situation, the ego vehicle makes an abnormal decision to drive directly off the road to avoid collision.

**5.1.5 Case Study V.** In Figure 9a, two surrounding vehicles are crashed in front of the green ego vehicle. Despite the collision, the ego vehicle maintains its course and attempts to pass the yellow

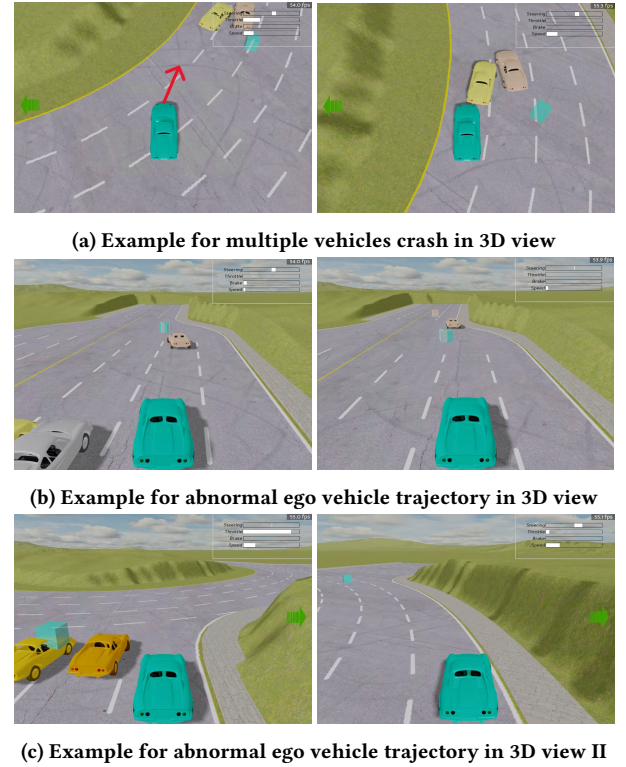


**Figure 9: Examples of safety violation from 3D view simulation**

surrounding vehicle, believing there is enough space on the left. Unfortunately, this leads to another collision involving multiple vehicles.

**5.1.6 Case Study VI.** Figure 9b indicates a **Merge** scenario, two surrounding vehicles collided beside the green ego vehicle, and a brown surrounding vehicle is moving forward in front of the ego vehicle. However, even though the brown vehicle has already moved far away, the ego vehicle still does not move, which causes a timeout issue.

**5.1.7 Case Study VII.** Figure 9c indicates a **Roundabout** scenario, initially, two yellow surrounding vehicles are moving on the left-hand side of the green ego vehicle, which is in the outermost lane of the road. They are preparing to enter the roundabout by slightly turning right. However, due to the close proximity of the surrounding vehicles, the ego vehicle oversteers and drives off the road.

From the case study, we observe that the ADSs under test can generally respond to the dynamic trajectory of a single surrounding vehicle in most of cases. However, in these scenarios with complex dynamic interactions among multiple surrounding vehicles, even when the ego vehicle responds promptly, it is still unable to avoid safety violations. We have identified these scenarios as potentially containing bugs in the autonomous driving model and have shared the corresponding videos and logs with the developers of MetaDrive

to support system improvement. More safety violation demos can be found in our anonymous repository <sup>1</sup>.

## 5.2 Comparison to Baselines (RQ2)

Table 3 shows the performance of MARL-OT and baseline methods in the IDM policy ADS across different scenarios. As indicated in RQ1, we selected the IDM policy for testing in RQ2 due to its demonstrated robustness. We observe that MARL-OT outperforms all other baseline methods across all metrics, with a specific improvement of up to 136.2% over Single-Agent RL. The GA and Random baselines identify very few safety violations in some scenarios.

Different methods show significant performance differences across various maps. In the **Merge** scenario, even the Random baseline achieves a 5.4% safety violation rate, as this scenario involves multiple vehicles entering a narrower road, increasing the likelihood of safety violations. In other words, the **Merge** scenario is easier to trigger safety violations and more dangerous. In this scenario, we observe that both the Single-Agent RL and MARL-OT nearly match each other's performance. GA also shows notable improvement, due to its evolutionary nature, which carries forward safety violations found in the initial generation throughout the process.

In less dangerous scenarios such as **Straight**, **Circular**, and **MIX**, the safety violation rate of the GA and Random baselines is under 1%, while RL-based online methods remain consistently stable. This reveals a disadvantage of GA: it tends to retain the chromosome representations that lead to safety violations. If no safety violations are found during the initial generation's random initialization, GA relies on random mutation and crossover, which cannot guarantee that evolution will approach the violation boundary. As a result, GA struggles to adapt quickly to scenarios. In contrast, online methods like RL can better adapt to the scenario and identify violations, highlighting the limitations of offline methods like GA in online testing scenarios.

When we look at the online testing method RL, although it remains stable in generating violations across different scenarios, without agent cooperation, single-agent RL still has a large gap with MARL-OT when generating safety violations involving multiple vehicles. The results also demonstrate that offline methods like GA and Random can only identify a limited number of safety violations, underscoring the challenge of detecting subtle errors in seemingly robust ADSs like IDM. This highlights the need for our approach, which generates scenarios involving multiple surrounding vehicles with complex interactions.

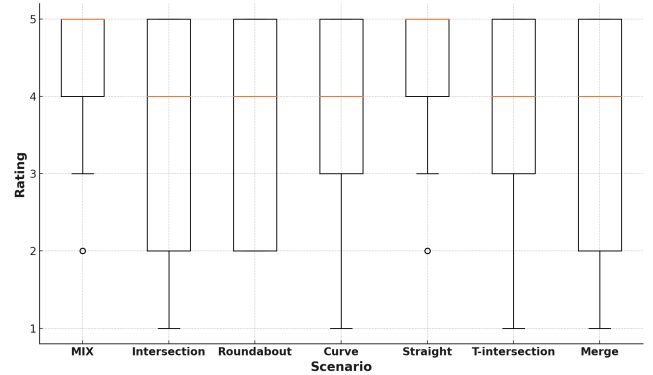
## 5.3 Realism of Generated Cases (RQ3)

Figure 10 shows the box plot of realism ratings from the user study, where the red line indicates the median rating in each scenario. We find that the median rating for all scenarios is above 4, indicating that our generated scenarios have high realism. However, there are still some outliers, and here we further analyze those outliers.

**5.3.1 Outlier Analysis I.** Figure 11 shows the outlier in the **MIX** scenario. Initially, the blue surrounding vehicle is stopped due to

**Table 3: Quantitative result of safety violation case generating efficiency for different methods, 'None' indicates TOP-5 cannot be found, best is marked in bold.**

Map Type	Metric	MARL-OT	GA	RL	Random
Straight	Violation Rate (%)	<b>10.1</b>	0.3	5.2	0.1
	TOP-5	<b>68.8</b>	None	120.4	None
Roundabout	Violation Rate (%)	<b>10.3</b>	1.9	5.1	2.2
	TOP-5	<b>69.2</b>	200.0	129.8	173.7
Merge	Violation Rate (%)	<b>11.1</b>	6.7	11.0	5.4
	TOP-5	<b>56.4</b>	88.0	58.2	114.2
T-Intersection	Violation Rate (%)	<b>11.1</b>	2.9	4.7	2.4
	TOP-5	<b>55.2</b>	141.3	105.8	194.3
Circular	Violation Rate (%)	<b>14.9</b>	0.2	7.8	0.6
	TOP-5	<b>36.8</b>	None	79.2	None
Intersection	Violation Rate (%)	<b>9.3</b>	1.8	8.2	1.7
	TOP-5	<b>38.6</b>	None	85.6	None
MIX	Violation Rate (%)	<b>13.0</b>	0.5	7.9	0.8
	TOP-5	<b>50.0</b>	None	72.6	None



**Figure 10: Boxplots for User Ratings on Different Scenarios with Outliers**

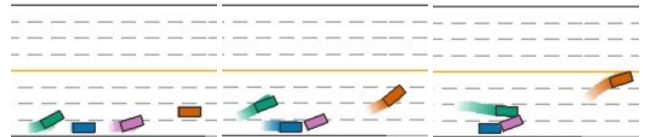


**Figure 11: Outlier in the MIX scenario**

the Driving Behavior Constraint defined in Section 3.5, as the green ego vehicle is close. The ego vehicle attempts to accelerate and change lanes to overtake. The pink surrounding vehicle is also initially stopped, but after a while, it begins to change lanes at a low speed. Once the pink vehicle moves slightly, the driving behavior constraint on the blue vehicle is no longer triggered, allowing it

<sup>1</sup><https://anonymous.4open.science/r/MARL-OT-E1B5>

to start moving. The abnormal behavior occurs when the pink vehicle suddenly stops, which appears unrealistic from the testers' perspective. Upon reviewing the log, it is clear that the pink vehicle triggered the side front action pattern, activating the brake condition. Since the pink vehicle was moving at a low speed, it could stop in a short time. Consequently, the ego vehicle failed to avoid the pink vehicle, resulting in a collision. This highlights the impact of our rule-based action pattern.

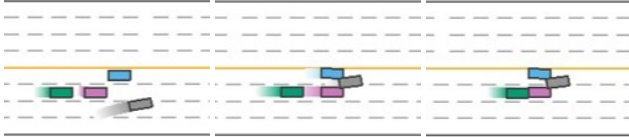


Figure 12: Outlier in the straight scenario

**5.3.2 Outlier Analysis II.** Figure 12 shows the outlier in the **Straight** scenario. The pink surrounding vehicle's driving behavior seems unrealistic, as it tries to intentionally block the green ego vehicle with a low speed. Even though another two surrounding vehicles collide around it, the pink vehicle continues to move at a low speed. Finally, the pink vehicle collides with those vehicles, and the ego vehicle collides with the pink vehicle. After checking the log, this could be explained by our Driving Behavior Constraint defined in Section 3.5. As the two vehicles collided in front of the pink vehicle and stopped there, this triggered the driving behavior constraint of the pink vehicle to avoid colliding with other vehicles, causing it to move at a very low speed in an attempt to stop. However, due to its motion, it cannot stop completely, which results in the appearance of intentionally blocking the ego vehicle.

## 6 DISCUSSION

In this work, we conduct an in-depth qualitative analysis of the latest simulator, MetaDrive. We use the built-in end-to-end driving models for evaluation: IDM, representing a rule-based model, and PPO, representing a learning-based model. Both are repetitive end-to-end learning models. Our approach is not limited to MetaDrive or end-to-end driving models alone; we plan to extend evaluation to other simulators, such as CARLA, and to multi-module driving systems, such as Baidu Apollo and Autoware.

Our primary focus is on detecting safety violations of the ego-vehicle in scenarios involving multiple surrounding vehicles, where the complex interplay among these vehicles can lead the ego-vehicle's ADS into unsafe behaviors. This is a challenging task that state-of-the-art testing methods have failed to address, as shown in our experiments. Detailed records of these safety violations have been reported to the MetaDrive developers to help identify root causes. Early detection of potential safety issues is crucial for real-world ADS development and has the potential to be adapted to other machine learning-enabled cyber-physical systems, where dynamic objects in the environment can present unpredictable yet hazardous scenarios.

## 7 CONCLUSION

In this paper, we present an innovative online testing method for generating safety violations involving multiple vehicles in ADS. Our approach combines a highly efficient multi-agent reinforcement learning (MARL) with a rule-based online fuzzer to produce realistic yet hazardous scenarios for the ego vehicle created by surrounding vehicles. Experiments show that MARL-OT detects up to 136.2% more safety violations than state-of-the-art methods. A user study further validates the realism of the generated scenarios. Future research will expand MARL-OT by replacing the rule-based fuzzer with a more efficient online fuzzer, allowing MARL-OT to explore the confined search space using MARL without rule constraints. We also plan to apply MARL-OT to other machine learning-enabled cyber-physical systems, such as autonomous UAV landing systems.

## REFERENCES

- [1] [n. d.]. Baidu Apollo team (2017), Apollo: Open Source Autonomous Driving, howpublished = <https://github.com/ApolloAuto/apollo>, note = Accessed: 2019-02-11.
- [2] Raja Ben Abdesslem, Annibale Panichella, Shiva Nejati, Lionel C Briand, and Thomas Stifter. 2018. Testing autonomous cars for feature interaction failures using many-objective search. In *Proceedings of the 33rd ACM/IEEE International Conference on Automated Software Engineering*. 143–154.
- [3] ApolloAuto. 2024. Apollo. <https://github.com/ApolloAuto/apollo>.
- [4] Earl T Barr, Mark Harman, Phil McMinn, Muzammil Shahbaz, and Shin Yoo. 2014. The oracle problem in software testing: A survey. *IEEE transactions on software engineering* 41, 5 (2014), 507–525.
- [5] Raja Ben Abdesslem, Shiva Nejati, Lionel C Briand, and Thomas Stifter. 2016. Testing advanced driver assistance systems using multi-objective search and neural networks. In *Proceedings of the 31st IEEE/ACM international conference on automated software engineering*. 63–74.
- [6] Michele Bertoncello and Dominik Wee. 2015. Ten ways autonomous driving could redefine the automotive world. *McKinsey & Company* 6 (2015).
- [7] Greg Brockman, Vicki Cheung, Ludwig Pettersson, Jonas Schneider, John Schulman, Jie Tang, and Wojciech Zaremba. 2016. OpenAI Gym. [arXiv:1606.01540](https://arxiv.org/abs/1606.01540) [cs.LG]. <https://arxiv.org/abs/1606.01540>
- [8] Li Chen, Penghao Wu, Kashyap Chitta, Bernhard Jaeger, Andreas Geiger, and Hongyang Li. 2024. End-to-end autonomous driving: Challenges and frontiers. *IEEE Transactions on Pattern Analysis and Machine Intelligence* (2024).
- [9] Kalyanmoy Deb, Samir Agrawal, Amrit Pratap, and Tanaka Meyarivan. 2000. A fast elitist non-dominated sorting genetic algorithm for multi-objective optimization: NSGA-II. In *Parallel Problem Solving from Nature PPSN VI: 6th International Conference Paris, France, September 18–20, 2000 Proceedings* 6. Springer, 849–858.
- [10] Yao Deng, Jiaohong Yao, Zhi Tu, Xi Zheng, Mengshi Zhang, and Tianyi Zhang. 2023. Target: Traffic rule-based test generation for autonomous driving systems. *arXiv preprint arXiv:2305.06018* (2023).
- [11] Yao Deng, Xi Zheng, Mengshi Zhang, Guannan Lou, and Tianyi Zhang. 2022. Scenario-based test reduction and prioritization for multi-module autonomous driving systems. In *Proceedings of the 30th ACM Joint European Software Engineering Conference and Symposium on the Foundations of Software Engineering*. 82–93.
- [12] Hamid Ebadi, Mahshid Helali Moghadam, et al. 2021. Efficient and effective generation of test cases for pedestrian detection-search-based software testing of Baidu Apollo in SVL. In *2021 IEEE International Conference on Artificial Intelligence Testing (AITest)*. IEEE, 103–110.
- [13] Shuo Feng, Haowei Sun, Xintao Yan, et al. 2023. Dense reinforcement learning for safety validation of autonomous vehicles. *Nature* 615, 7953 (2023).
- [14] Fitash Ul Haq, Donghwan Shin, and Lionel Briand. 2022. Many-Objective Reinforcement Learning for Online Testing of DNN-Enabled Systems. *arXiv preprint arXiv:2210.15432* (2022).
- [15] Yuqi Huai, Sumaya Almanee, Yuntianyi Chen, Xiafa Wu, Qi Alfred Chen, and Joshua Garcia. 2023. sceno RITA: Generating Diverse, Fully-Mutable, Test Scenarios for Autonomous Vehicle Planning. *IEEE Transactions on Software Engineering* (2023).
- [16] Longting Jiang, Ruixuan Wei, and Dong Wang. 2023. UAVs rounding up inspired by communication multi-agent depth deterministic policy gradient. *Applied Intelligence* 53, 10 (2023), 11474–11489.
- [17] Mark Koren, Saud Alsaif, Ritchie Lee, and Mykel J Kochenderfer. 2018. Adaptive stress testing for autonomous vehicles. In *2018 IEEE Intelligent Vehicles Symposium*. IEEE.

- [18] Mark Koren, Ahmed Nassar, and Mykel J Kochenderfer. 2021. Finding failures in high-fidelity simulation using adaptive stress testing and the backward algorithm. In *2021 IEEE/RSJ International Conference on Intelligent Robots and Systems (IROS)*. IEEE.
- [19] Fred Lambert. 2016. Understanding the fatal tesla accident on autopilot and the nhtsa probe. *Electrek*, July 1 (2016), 1.
- [20] Guanpeng Li, Yiran Li, Saurabh Jha, et al. [n. d.]. Av-fuzzer: Finding safety violations in autonomous driving systems. In *2020 IEEE 31st international symposium on software reliability engineering (ISSRE)*.
- [21] Quanyi Li, Zhenghao Peng, Lan Feng, Qihang Zhang, Zhenghai Xue, and Bolei Zhou. 2022. Metadrive: Composing diverse driving scenarios for generalizable reinforcement learning. *IEEE transactions on pattern analysis and machine intelligence* 45, 3 (2022), 3461–3475.
- [22] Linfeng Liang, Yao Deng, Kye Morton, Valtteri Kallinen, Alice James, Avishkar Seth, Endrowednes Kuantama, Subhas Mukhopadhyay, Richard Han, and Xi Zheng. 2023. RLaGA: A Reinforcement Learning Augmented Genetic Algorithm For Searching Real and Diverse Marker-Based Landing Violations. *arXiv preprint arXiv:2310.07378* (2023).
- [23] Guannan Lou, Yao Deng, et al. 2022. Testing of autonomous driving systems: where are we and where should we go?. In *Proceedings of the 30th ACM Joint European Software Engineering Conference and Symposium on the Foundations of Software Engineering*. 31–43.
- [24] Ryan Lowe, Yi I Wu, Aviv Tamar, Jean Harb, OpenAI Pieter Abbeel, and Igor Mordatch. 2017. Multi-agent actor-critic for mixed cooperative-competitive environments. *Advances in neural information processing systems* 30 (2017).
- [25] Chengjie Lu, Yize Shi, et al. 2022. Learning configurations of operating environment of autonomous vehicles to maximize their collisions. *IEEE Transactions on Software Engineering* 49, 1 (2022), 384–402.
- [26] Yuteng Lu, Kaicheng Shao, Weidi Sun, and Meng Sun. 2022. RGChaser: A RL-guided Fuzz and Mutation Testing Framework for Deep Learning Systems. In *2022 9th International Conference on Dependable Systems and Their Applications (DSA)*. IEEE, 12–23.
- [27] Yixing Luo, Xiao-Yi Zhang, et al. 2021. Targeting requirements violations of autonomous driving systems by dynamic evolutionary search. In *2021 36th IEEE/ACM International Conference on Automated Software Engineering (ASE)*. IEEE, 279–291.
- [28] MetaDrive Developers. 2024. MetaDrive Documentation. <https://metadrive-simulator.readthedocs.io/en/latest/> Accessed: 2024-11-12.
- [29] NHTSA. 2022. NHTSA Report. <https://www.nhtsa.gov/sites/nhtsa.gov/files/811731.pdf> Retrieved May 11, 2022.
- [30] NHTSA. 2022. Pre-crash scenarios in NHTSA. [https://www.nhtsa.gov/sites/nhtsa.gov/files/pre-crash\\_scenario\\_typologyfinal\\_pdf\\_version\\_5-2-07.pdf](https://www.nhtsa.gov/sites/nhtsa.gov/files/pre-crash_scenario_typologyfinal_pdf_version_5-2-07.pdf) Retrieved May 11, 2022.
- [31] National People's Congress of China. 2007. Constitution of the People's Republic of China. [http://www.npc.gov.cn/zgrdw/englishnpc/Law/2007-12/05/content\\_1381965.htm](http://www.npc.gov.cn/zgrdw/englishnpc/Law/2007-12/05/content_1381965.htm) Accessed: 2024-11-13.
- [32] Annibale Panichella, Fitsum Meshesha Kifetew, and Paolo Tonella. 2015. Reformulating branch coverage as a many-objective optimization problem. In *2015 IEEE 8th international conference on software testing, verification and validation (ICST)*. IEEE, 1–10.
- [33] Tabea Schmidt and Alexander Pretschner. 2022. StellaUAV: A Tool for Testing the Safe Behavior of UAVs with Scenario-Based Testing (Tools and Artifact Track). In *2022 IEEE 33rd International Symposium on Software Reliability Engineering (ISSRE)*.
- [34] John Schulman, Filip Wolski, Prafulla Dhariwal, Alec Radford, and Oleg Klimov. 2017. Proximal policy optimization algorithms. *arXiv preprint arXiv:1707.06347* (2017).
- [35] Richard S Sutton and Andrew G Barto. 2018. *Reinforcement learning: An introduction*. MIT press.
- [36] Inc. Tesla. 2024. Autopilot. [https://www.tesla.com/en\\_AU/autopilot](https://www.tesla.com/en_AU/autopilot) Accessed: 2024-11-13.
- [37] Haoxiang Tian, Yan Jiang, et al. 2022. MOSAT: finding safety violations of autonomous driving systems using multi-objective genetic algorithm. In *ESEC/FSE 2022*. 94–106.
- [38] Martin Treiber, Ansgar Hennecke, and Dirk Helbing. 2000. Congested traffic states in empirical observations and microscopic simulations. *Physical review E* 62, 2 (2000), 1805.
- [39] Oriol Vinyals, Igor Babuschkin, Wojciech M Czarnecki, Michaël Mathieu, Andrew Dudzik, Junyoung Chung, David H Choi, Richard Powell, Timo Ewalds, Petko Georgiev, et al. 2019. Grandmaster level in StarCraft II using multi-agent reinforcement learning. *nature* 575, 7782 (2019), 350–354.
- [40] Joachim Wegener and Oliver Bühler. 2004. Evaluation of different fitness functions for the evolutionary testing of an autonomous parking system. In *Genetic and Evolutionary Computation—GECCO 2004: Genetic and Evolutionary Computation Conference, Seattle, WA, USA, June 26–30, 2004. Proceedings, Part II*. Springer Berlin Heidelberg, 1400–1412.
- [41] Ziyuan Zhong, Gail Kaiser, and Baishakhi Ray. 2022. Neural network guided evolutionary fuzzing for finding traffic violations of autonomous vehicles. *IEEE Transactions on Software Engineering* (2022).